IL-2 enhances effector function but suppresses follicular localization of CD8$^+$ T cells in chronic infection

Yaping Chen[1,2,9], Pengcheng Zhou[3,4,6,*], Patrick Marc Gubser[5], Yew Ann Leong[1], Jing He[6], Yunbo Wei[7], Fadzai Victor Makota[3], Mehrdad Pazhouhandeh[4], Ting Zheng[3,7], Joseph Yunis[3,4,8], Zhanguo Li[6], Axel Kallies[5,*], Di Yu[1,3,4,8,10,*]

1 Department of Biochemistry, School of Biomedical Sciences, Biomedical Discovery Institute, Monash University, Clayton, Victoria, Australia

2 Oujiang Laboratory (Zhejiang Lab for Regenerative Medicine, Vision and Brain Health), Wenzhou, Zhejiang, P.R. China

3 Immunology and Infectious Disease Division, John Curtin School of Medical Research, The Australian National University, Canberra, Australian Capital Territory, Australia

4 Frazer Institute, Faculty of Medicine, The University of Queensland, Brisbane, Queensland, Australia

5 The Peter Doherty Institute for Infection and Immunity, Department of Microbiology and Immunology, The University of Melbourne, Parkville, Victoria, Australia

6 Department of Rheumatology & Immunology, Peking University People's Hospital, Beijing, China

7 Laboratory of Immunology for Environment and Health, Shandong Analysis and Test Center, Qilu University of Technology (Shandong Academy of Sciences), Jinan, Shandong, China

8 Ian Frazer Centre for Children's Immunotherapy Research, Children's Health Research Centre, Faculty of Medicine, The University of Queensland, Brisbane, Queensland, Australia

9 These authors contributed equally

10 Lead corresponding author

28 *Correspondence:

29 D.Y. (di.yu@uq.edu.au)

30 A.K. (axel.kallies@unimelb.edu.au)

31 P.Z. (pzhou@rockefeller.edu)

32

Summary

Cytotoxic $CD8^+$ T cells, essential in combating viral infections and cancer, become dysfunctional from prolonged antigen exposure. Precursors of exhausted T (T_{PEX}) cells are pivotal in sustaining immune responses in chronic diseases and mediating immunotherapy efficacy. They also control viral infection within B-cell follicles, facilitated by CXCR5 expression. How cytokines regulate T_{PEX} cell fate and follicular entry is not well understood. We reveal that IL-2 treatment enhances $CD8^+$ T cell effector functions in chronic LCMV infection but hinders $CXCR5^+$ T_{PEX} cell formation and infection control within B-cell follicles. Mechanistically, IL-2 suppresses T_{PEX} cell differentiation in a STAT5 and BLIMP1-dependent manner. Using an IL-2 fusion protein targeting CD122, we shifted the differentiation towards $CX3CR1^+$ T cells with increased effector function. Clinical observations with low-dose IL-2 in autoimmune disease confirmed IL-2's inhibitory effect on $CXCR5^+$ T_{PEX} cells, underscoring IL-2's crucial regulatory role and therapeutic potential in modulating T_{PEX} and effector T cell generation.

Keywords:

Interleukin-2, LCMV, follicular infection, T_{PEX}, CXCR5, STAT5

INTRODUCTION

$CD8^+$ T cells play a critical role in eliminating virally infected and malignant cells. In chronic infection and cancer, antigen-specific $CD8^+$ T cells persistently exposed to antigen gradually reduce their ability to produce effector cytokines and proliferative capacity. This process is paralleled by the upregulation of inhibitory receptors or checkpoints such as programmed cell death protein 1 (PD-1), T cell immunoglobulin and mucin domain 3 (TIM-3) and lymphocyte-activation gene 3 (LAG3). Although such cellular reprogramming is necessary to restrain $CD8^+$ T cells-mediated immunopathology, reduced functionality in $CD8^+$ T cells impairs the clearance of infection or prevention of tumor growth. This process is referred to as T cell exhaustion (Blank et al., 2019; Hashimoto et al., 2018; McLane et al., 2019).

PD-1^+ exhausted $CD8^+$ T cells are heterogenous and contain a population of cells known as progenitors or precursors of exhausted T (T_{PEX}) cells. These cells retain the capacity to self-renew while also giving rise to exhausted effector T (T_{EX}) cells as we and others have shown (He et al., 2016b; Im et al., 2016; Leong et al., 2016; Utzschneider et al., 2016; Wu et al., 2016). T_{PEX} cells also mediate the response to immune checkpoint blockade (ICB) therapies that inhibit PD-1/PD-Ligand 1 (PD-L1) interactions and thus amplify anti-viral and anti-tumor immunity in mice and humans (Eberhardt et al., 2021; Huang et al., 2022; Im et al., 2016; Siddiqui et al., 2019; Utzschneider et al., 2016). T_{PEX} cells express the chemokine receptor CXCR5, which facilitates their migration to B-cell follicles where they contribute to the suppression of infection (He et al., 2016b; Leong et al., 2016). This is important as B-cell follicles act as reservoirs for certain viruses, such as Epstein–Barr virus (EBV) in memory B cells and Human Immunodeficiency Virus (HIV) in follicular helper T (T_{FH}) cells (Collins et al., 2023; Leong et al., 2016; Mylvaganam et al., 2017; Petrovas et al., 2017). Therefore, CXCR5-expressing T_{PEX} cells are critical in suppressing the infection in B-cell follicles (Yu and Ye, 2018).

T cell exhaustion is controlled by a network of transcriptional regulators induced by T cell receptor (TCR) stimulation-induced transcription factors, in particular NFATC1, TOX and IRF4 drive the sustained expression of inhibitory receptors and contribute to the downregulation of effector function (Alfei et al., 2019; Khan et al., 2019; Man et al., 2017;

Martinez et al., 2015; Scott et al., 2019; Seo et al., 2019; Yao et al., 2019). The generation and maintenance of T_{PEX} cells, on the other hand, are specifically controlled by transcription factors such as TCF1, MYB, ID3 and BCL6 while T_{EX} cells differentiation is promoted by BLIMP1(Gautam et al., 2019; He et al., 2016b; Im et al., 2016; Leong et al., 2016; Tsui et al., 2022; Utzschneider et al., 2016; Wu et al., 2016). However, extracellular signals that regulate T_{PEX} and T_{EX} cell differentiation and maintenance are less understood. We and others have shown that TGFβ plays a key role in maintaining T_{PEX} cell function and identity (Gabriel et al., 2021; Hu et al., 2022; Ma et al., 2022). Furthermore, both T_{FH} cells-derived cytokine interleukin-21 (IL-21) and the alarmin IL-33 are necessary to maintain T_{PEX} cells and sustain effector $CD8^+$ T cell function in chronic infection (Marx et al., 2023; Yu et al., 2022; Zander et al., 2022). Finally, IL-2, in combination with ICB, was shown to direct T_{PEX} cells to generate transitory effector $CD8^+$ T cells and improve antiviral and antitumor activities (Codarri Deak et al., 2022; Hashimoto et al., 2022; Ren et al., 2022; Tichet et al., 2023; West et al., 2013). However, the precise function of IL-2 in regulating T cell exhaustion is not fully understood.

To better understand how IL-2 regulates T_{PEX} cell differentiation and function, we investigated the impact and molecular mechanisms of treatment with IL-2 or a clinical-grade IL-2 fusion protein specifically targeting the IL-2 receptor β chain (CD122) in chronic LCMV infection. IL-2 treatment increased the generation of CX3CR1+ T_{EX} cells with enhanced effector function without disrupting the self-renewal capacity of T_{PEX} cells both in mouse and human. At the same time, IL-2 treatment resulted in downregulation of CXCR5 expression on T_{PEX} cells, their exclusion from B-cell follicles and impaired viral clearance from these sites. Furthermore, increased IL-2 signaling during the early stages of the immune response strongly suppressed T_{PEX} cell generation. Mechanistically, IL-2 exerted its effects in a STAT5- and BLIMP1-dependent manner. Overall, our data show that IL-2 treatment can broadly modulate the balance between effector T cells and T_{PEX} cells and excert differential effects on viral clearance.

RESULTS

IL-2 treatment promotes $CD8^+$ T effector expansion during chronic infection

110 IL-2 is an approved immunotherapeutic agent for cancer (Dutcher et al., 2014). It's precise
111 mechanism of action is not fully understood. To elucidate how IL-2 affects exhausted
112 $CD8^+$ T cell maintenance and function, wild-type C57BL/6 mice were infected with LCMV
113 Docile (10^6 plaque-forming units, PFU), which induces chronic infection and robust T cell
114 exhaustion. Mice were treated with PBS or low-to-medium dose of recombinant human
115 IL-2 (30,000 international units, IU (Blattman et al., 2003; He et al., 2016a; West et al.,
116 2013)) daily from day 10 to 14 post-infection before analysis on day 15 (**Figure 1A**). IL-2
117 treatment elevated $CD8^+$ T cell numbers and increased $CD8^+/CD4^+$ T cell ratios (**Figure**
118 **1B**). Furthermore, numbers of activated $CD8^+$ T cells ($CD44^{high}CD62L^-$) and their effector
119 function as measured by Granzyme B expression were significantly enhanced by IL-2
120 treatment (**Figure 1C, D**). In agreement with previous studies (Blattman et al., 2003; Zhou
121 et al., 2021), we found that IL-2 treatment significantly increased both the frequencies
122 and numbers of LCMV-specific $CD8^+$ T cells as measured by staining with H-$2D^b$ LCMV
123 GP_{33} tetramers (**Figure 1E**). We did not observe an expansion of regulatory (T_{REG}) cells
124 by this dose of IL-2 treatment (data not shown), presumably due to the high numbers of
125 activated effector T cells (Humblet-Baron et al., 2016; Zhou et al., 2021). We next
126 examined the impact of IL-2 treatment on the generation of $TCF1^+CXCR5^+$ T_{PEX} and
127 $TCF1^-CXCR5^-$ T_{EX} cells. IL-2 treatment increased the total numbers of T_{EX} cells by more
128 than two-fold (**Figure 1F**). In contrast, IL-2 treatment reduced the frequencies of T_{PEX} cells
129 within GP_{33} tetramer$^+$ $CD8^+$ T cells by more than two-fold although their numbers
130 remained largely unchanged (**Figure 1F**). Overall, IL-2 treatment enhanced effector T cell
131 expansion in chronic infection.

132

133 **IL-2 alters tissue localization of $CD8^+$ T cells and viral reservoirs in chronic infection**

134 Previous studies reported that a short period of IL-2 treatment, despite enhancing $CD8^+$
135 T effector function, was insufficient to significantly reduce viral loads (Blattman et al.,
136 2003; Zhou et al., 2021). LCMV preferentially infects myeloid cells expressing high levels
137 of α-Dystroglycan (α-DG), the cellular receptor for LCMV (Kunz et al., 2001; Oldstone and
138 Campbell, 2011), but it also infects lymphocytes including $CD4^+$ T cells (Leong et al.,
139 2016). Immunofluorescent microscopy of splenic tissue using the antibody (VL4) to LCMV

140 nucleoprotein revealed that IL-2 treatment resulted in an altered distribution of VL4$^+$
141 LCMV reservoirs towards B220$^+$ B-cell follicles (**Figure 2A**). To examine whether IL-2
142 treatment influenced the distribution of virus in the B-cell follicle and the T-cell zone, we
143 deployed a flow cytometry-based method previously developed (Leong et al., 2016).
144 Treatment with IL-2, in a dose-dependent manner, reduced numbers of virus-infected
145 CXCR5^{low}CD44$^+$ non-T_{FH} effector CD4$^+$ T cells, which primarily reside in the T-cell zone,
146 whereas the numbers of virally infected CXCR5^{high}CD44$^+$ T_{FH} cells, which mostly reside
147 in B-cell follicles, remained unchanged. As a consequence, the LCMV reservoir was
148 biased towards the B-cell follicle, indicated by a two-fold increase in the ratio of infected
149 T_{FH}/non-T_{FH} cells at the highest dose of IL-2 treatment (**Figure 2B**).

150 T_{PEX} cells that express CXCR5 have access to the B-cell follicle and contribute to viral
151 control (Collins et al., 2023; Leong et al., 2016; Petrovas et al., 2017). The altered
152 distribution of LCMV reservoirs, however, suggested that IL-2 treatment prevents access
153 of CD8$^+$ T cells to B-cell follicles. Indeed, IL-2 treatment significantly reduced CXCR5
154 expression on T_{PEX} cells (**Figure 2C**). In line with this observation, immunofluorescent
155 imaging of splenic tissue sections revealed a drastic reduction of CD8$^+$ T cells in the B-
156 cell follicles in IL-2-treated mice compared with that of PBS-treated control mice (**Figure**
157 **2D**).

158 Systemic administration of IL-2 may control CD8$^+$ T cell activation and differentiation
159 directly or indirectly. We therefore assessed the direct impact of IL-2 *in vitro*. Stimulation
160 of human CD8$^+$ T cells with anti-CD3/CD28 and cytokines TGFβ, IL-12, and IL-23 was
161 shown to promote CXCR5 expression (Mylvaganam et al., 2017). In lijne with that
162 observation, we and others found that TGFβ supported T_{PEX} cell generation and
163 maintenance (Gabriel et al., 2021; Hu et al., 2022; Ma et al., 2022). We therefore
164 optimized a culture condition whereby naïve mouse OT-I CD8$^+$ T cells that carry a
165 transgenic TCR-specific to ovalbumin (OVA) antigen were stimulated with splenocytes
166 pulsed with SIINFEKL peptide in the presence or absence of TGFβ and IL-6, with or
167 without IL-2. The combination of TGFβ and IL-6 induced CXCR5 expression on OT-I T
168 cells. In contrast, the addition of IL-2 in the culture diminished CXCR5 expression by
169 about three-fold (**Figure 2E**). Overall, these results suggest that IL-2 induces signaling
170 that favors the generation of CXCR5$^-$ T_{EX} cells over CXCR5$^+$ T_{PEX} cells in CD8 T cells.

171

172 **An IL-2-STAT5-BLIMP1 axis regulates the balance of effector and T_{PEX} generation**

173 To better understand the impact of IL-2 on T_{PEX} and T_{EX} cell generation, we performed
174 Gene Set Enrichment Analysis (GSEA) of CXCR5$^+$ T_{PEX} cells compared to CXCR5$^-$ T_{EX}
175 cells (Leong et al., 2016). This analysis indicated downregulation of IL-2-STAT5 signaling
176 in CXCR5$^+$ T_{PEX} cells (**Suppl. Figure 1A**), suggesting that IL-2 negatively impacts the
177 generation or function of CXCR5$^+$ T_{PEX} cells. The IL-2 receptor is a heterotrimeric protein
178 complex composed of three subunits: the α subunit CD25 encoded by *Il2ra*, the β subunit
179 CD122 encoded by *Il2rb*, and the common γ chain CD132 encoded by *Il2rg* (Boyman and
180 Sprent, 2012). Transcriptomic analysis indicated that *Il2ra* and *Il2rb* were lower in
181 CXCR5$^+$ T_{PEX} population, whereas *Il7r* was higher, compared with CXCR5$^-$ T_{EX} cells
182 (**Suppl. Figure 1B,C**). Flow cytometric analysis showed that the expression of CD122 on
183 CXCR5$^+$ T_{PEX} was significantly lower than that on CXCR5$^-$ T_{EX} cells, while CD25 protein
184 was minimally expressed on both populations (**Figure 3A**). Notably, the treatment of IL-2
185 in mice with LCMV infection pronouncedly increased CD122 expression and modestly
186 increased CD25 expression on T_{PEX} cells, whereas such effects were not observed in T_{EX}
187 cells (**Figure 3B** and **Suppl. Figure 1D**).

188 The phosphorylation of STAT5 (pSTAT5) is a major signaling event induced by IL-2
189 (Boyman and Sprent, 2012). IL-2 treatment increased the pSTAT5 level in CXCR5$^+$ T_{PEX}
190 cells but not in CXCR5$^-$ T_{PEX} cells (**Figure 3C**). To directly test the impact of STAT5
191 signaling, we transduced CD45.2 TCR transgenic P14 T cells that are specific for the
192 LCMV GP_{33-41} epitope with the retrovirus expressing a constitutively activated version of
193 STAT5b (STAT5b-CA) or an empty viral vector control (Johnston et al., 2012).
194 Transduced P14 T cells were then transferred into congenically marked CD45.1 recipient
195 mice followed by LCMV Docile infection (**Figure 3D**). Similar to the effects of IL-2
196 treatment and in line with a recent report (Beltra et al Immunity 2023), STAT5b-CA
197 overexpression led to an increase in total P14 cells by about three-fold compared to
198 controls (**Figure 3E**). Importantly, the constitutive activation of the STAT5 signaling in
199 P14 cells favored the generation of CXCR5$^-$ T_{EX} over CXCR5$^+$ T_{PEX} cells *in vivo* (**Figure**
200 **3F**).

201 CXCR5$^+$ T_{FH} cells and CXCR5$^+$ T_{PEX} cells share a similar transcriptional program for their
202 generation whereby both are promoted by transcription factors TCF1 and BCL6 and
203 suppressed by BLIMP1 and ID2 (Kallies et al., 2020; Vinuesa et al., 2016). We and others
204 previously reported that IL-2/STAT5 signaling induces the expression of B lymphocyte-
205 induced maturation protein-1 (BLIMP1, encoded by *Prdm1*), a negative regulator of *Cxcr5*
206 transcription (Johnston et al., 2009; Leong et al., 2016; Xin et al., 2016). We therefore
207 examined the roles of BLIMP1 in regulating the differentiation of CXCR5$^+$ T_{PEX} cells in
208 response to IL-2. First, we generated mixed bone marrow chimeric mice containing cells
209 from mice carrying a T cell-specific ablation of Blimp1 (*Prdm1*$^{flox/flox}$*Lck*^{Cre}) and cells from
210 congenically marked wildtype mice, mixed at a 1:1 ratio. These chimeras were infected
211 with LCMV Docile, treated with IL-2 or PBS from day 10 to day 14 and analyzed on day
212 15 (**Figure 3G**). As expected, we observed larger proportions of CXCR5$^+$ T_{PEX} cells in
213 BLIMP1-deficient (~30%) compared to control (~15%) CD8$^+$ T cells. Notably, IL-2
214 treatment further reduced the CXCR5$^+$ T_{PEX} cell percentages from ~15% to ~6% in control
215 CD8$^+$ T cells but did not reduce T_{PEX} cell frequencies in BLIMP1-deficient CD8$^+$ T cells,
216 which remained as ~30% (**Figure 3H**). Taken together, our results indicate that the IL-2-
217 STAT5-BLIMP1 axis plays a critical role in regulating the generation of CXCR5$^+$ T_{PEX} cells
218 in response to IL-2 treatment in chronic infection.

219

220 **An IL-2 fusion protein regulates the balance of effector and T_{PEX} cell generation**

221 IL-2 fusion proteins that increase the half-life or bioavailability of IL-2 have recently been
222 shown to be promising tools in cancer immunotherapy (Beltra et al., 2023; Codarri Deak
223 et al., 2022; Hashimoto et al., 2022; Tichet et al., 2023). To specifically assess the role of
224 the IL-2-CD122 axis in regulating the generation of T_{PEX} cells, we examined the effects of
225 a novel IL-2 fusion protein, ANV410, that selectively targets CD122. Consistent with the
226 CD122-specific activity, treatment of naïve mice with ANV410 resulted in a dramatic
227 expansion of CD44$^+$ memory CD8$^+$ T cells, and NK cells, without affecting T_{REG} cells
228 (**Suppl. Figure 2**). We next treated mice chronically infected with LCMV Docile (8-12
229 days post infection), which had received LCMV-specific P14 T cells (Regimen A, **Figure**
230 **4A**). Total CD8$^+$ as well as P14 T cells expanded substantially in response to ANV410

231 (**Figure 4B**). We also observed a significant increase in the percentage and numbers of
232 CX3CR1$^+$ T_{EX} cells (**Figure 4C**), which harbor the highest functional capacity among
233 exhausted T cells (Hudson et al., 2019; Zander et al., 2019). Consistent with this
234 observation, we also found larger numbers of P14 T cells expressing Granzyme B (**Figure**
235 **4D**). In contrast, the percentages of T_{PEX} cells in P14 T cells declined while their numbers
236 remained unchanged (**Figure 4E**), which was consistent with the results from IL-2
237 treatment (**Figure 2E**). To examine the effects of the IL-2 fusion protein on the generation
238 of T_{PEX} cells, we treated mice with ANV410 during the first 5 days post infection (Regimen
239 B, **Figure 4A**). Strikingly, early ANV410 treatment dramatically impaired the expansion of
240 P14 T cells (**Figure 4F**) and abrogated T_{PEX} cell development almost completely both in
241 the P14 and polyclonal PD-1$^+$ CD8 T cell compartment (**Figure 4G, H**), suggesting that
242 increased IL-2 signaling early during infection is detrimental to T_{PEX} cell development and
243 function.

244

245 **IL-2 treatment reduces CXCR5$^+$ T_{PEX} cells in humans**

246 Finally, we asked whether IL-2 treatment in humans could regulate T_{PEX} cells. We took
247 advantage of immunological profiling data that we previously collected in a clinical trial of
248 low-dose IL-2 therapy in patients with systemic lupus erythematosus (SLE). In this clinical
249 trial, patients were treated with three two-week cycles of 1,000,000 IU recombinant
250 human IL-2 every other day (**Figure 5I**) (He et al., 2016a). The results demonstrated that
251 low-dose IL-2 treatment significantly reduced human CXCR5$^+$ T_{PEX} cells in the blood after
252 three cycles of low-dose IL-2 therapy (**Figure 5J**); this is in agreement with the
253 observation of suppression of CXCR5 expression on CD8$^+$ T cells by IL-2 treatment in
254 the mouse model of LCMV chronic infection (**Figure 2C**). Overall, our data in both mice
255 and humans indicate that increased IL-2 signaling via CD122 during early stages of the
256 infection can impair the generation of T_{PEX} cells, while a short period of therapeutic IL-2
257 treatment at later stages of the infection increases the differentiation of effector cells from
258 T_{PEX} cells without impacting their self-renewal capacity.

259

260 **DISCUSSION**

261 Upon chronic antigen exposure, $CD8^+$ T cells upregulate the expression of inhibitory
262 receptors including PD-1. $PD\text{-}1^+$ T cells in chronic infection are heterogenous, containing
263 $TCF1^+$ T_{PEX} cells that undergo self-renewal but also give rise to $TCF1^-$ T_{EX} cells that lack
264 long-term proliferative capacity (He et al., 2016b; Huang et al., 2022; Im et al., 2016;
265 Leong et al., 2016; Utzschneider et al., 2016; Wu et al., 2016). Critically, T_{PEX} cells
266 mediate the proliferative burst in response to PD-1 immune checkpoint inhibition, which
267 induces the differentiation of $CX3CR1^+$ effector-like T_{EX} cells, which display the highest
268 effector function and antiviral activity and closely correlate with positive response to
269 therapeutic ICB in cancer (Hudson et al., 2019; Yan et al., 2018; Zander et al., 2019).
270 Maintaining a balance between self-renewal, effector function and terminal exhaustion
271 underlying by these functional subsets is essential to sustain cytotoxic killing while
272 restraining immunopathology at the same time (Blank et al., 2019; Hashimoto et al., 2018;
273 Kallies et al., 2020; McLane et al., 2019). Our results, together with studies published
274 recently (Beltra et al., 2023; Codarri Deak et al., 2022; Hashimoto et al., 2022; Liu et al.,
275 2021; Ren et al., 2022; Sun et al., 2023) suggest that regulating the T_{EX} and T_{PEX} cell
276 balance is a central role of IL-2 and the downstream STAT5-BLIMP1 axis. Importantly,
277 IL-2 promoted the generation of $CX3CR1^+$ effector-like T_{EX} cells without compromising
278 the self-renewal capacity of T_{PEX} cells.

279 IL-2 signaling is mediated by both the high affinity receptor IL-2Rα (CD25) and the
280 medium affinity receptor IL-2Rβ (CD122). Their individual contribution, however, is
281 dependent on their respective expression levels as well as the dose of IL-2. We found
282 that treatment with native IL-2 resulted in the upregulation of CD122 and induced
283 feedforward signaling. Consistent with this observation, the IL-2 fusion protein ANV410
284 that selectively targets CD122 but not CD25 induced the generation of CX3CR1 effector-
285 like T_{EX} cells, overall suggesting that CD122 is the main mediator of IL-2 effects on T_{PEX}
286 cells. These results align well with recent studies, which showed that CD122-dependent
287 signals drive terminal differentiation of $CD8^+$ T cells (Beltra et al., 2016) and CD122-
288 biased IL-2 agonism in the combination with ICB promoted $CD8^+$ T cell effector function
289 (Codarri Deak et al., 2022). Our results, however, do not preclude the possibility that IL-
290 2 treatment can induce signaling through CD25 as reported (Hashimoto et al., 2022).
291 Thus, IL-2 signaling is likely to be context-dependent. This notion is also highlighted by

292 our data showing that early, in contrast to late, treatment with the IL-2 fusion protein
293 ANV410 abrogated T_{PEX} cell development and impaired the expansion of antigen-specific
294 $CD8^+$ T cells.

295 Recent advancement in our understanding of the central role of IL-2 in the regulation of
296 $CD8^+$ T cell expansion and function has reinvigorated the enthusiasm for IL-2-based
297 immunotherapy in infection and cancer. Indeed, IL-2 and IL-2 fusion proteins have
298 emerged as powerful modulators that may promote viral clearance or tumor control.
299 Nevertheless, more work is required to understand the impact of IL-2 in a therapeutic
300 setting on the function of T_{PEX} cells and thus the long-term maintenance of $CD8^+$ T cell
301 responses in chronic infection and in cancer. Furthermore, the facts that IL-2 signaling
302 modulated the localization of $CD8^+$ T cells and altered the distribution of viral reservoirs
303 which may have implications for people living with HIV or experiencing EBV active
304 infection. Thus, further work is needed to dissect the therapeutic potential of IL-2. Taken
305 together, the development of IL-2-based immunotherapies should not only target the
306 correct receptor subunit but also consider T cell differentiation state and localization.
307

Acknowledgments

We acknowledge the Imaging and Cytometry Facility at the John Curtin School of Medical Research, The Australian National University and Flowcores at Monash University and Doherty Institute for technical support. We thank Shane P. Crotty (La Jolla Institute for Immunology) for STAT5b-CA and control vectors, William S Foster and James A. Harker (Imperial College London) for the advice on human studies. We thank ANAVEON for the supply of AN410.

Funding

Australian National Health and Medical Research Council (NHMRC) project GNT1085509 (DY), GNT2004333 (AK) and Leader Fellowship GNT2009554 (DY)
National Natural Science Foundation of China (NSFC) project 82071792 (YW)
Natural Science Foundation of Shandong Province 2021ZDSYS12 (YW)
Swiss National Research Foundation fellowship (PMG)

Author Contributions

Conceptualization: DY and AK
Supervision: DY, AK and ZL
Data curation: YC, PZ, PMG, YAL, JH, YW, FVM, TZ, and JY
Formal analysis: PZ, YC, PMG, YAL, YW and MP
Funding acquisition: DY, AK, PMG and YW
Writing, review and editing: DY, AK, PZ, YC and PMG

Declaration of Interests

The authors declare no conflicts of interests.

333 **Figure legends**

334

335 **Figure 1. IL-2 treatment promotes CD8+ T effector expansion during chronic**
336 **infection.**

337 (**A**) Schematic showing C57BL/6 mice chronically infected with LCMV Docile and
338 receiving intraperitoneal treatment of 30,000 IU recombinant human IL-2 daily from day
339 10 to 14 post infection, followed by the analyses on day 15. (**B**) Quantification showing
340 CD4/CD8 ratio and the numbers of $CD8^+$ T cells in the spleen. Cells were gated on $7AAD^-$
341 $B220^-$ $TCR\beta^+CD8^+$ or $CD4^+$ cells using flow cytometry. (**C**,**D**) Representative FACS plots
342 and statistics showing $CD44^{high}CD62L^{low}$ effector (C) and the expression of Granzyme B
343 (D) in total $CD8^+$ T cells in mice treated with PBS or IL-2. (**E, F**) Representative FACS
344 plots and quantification showing the frequencies and numbers of H-2Db LCMV GP_{33}
345 tetramer-specific $CD8^+$ T cells (E) and the frequencies and numbers of $CXCR5^-TCF1^-$ T_{EX}
346 cells and $CXCR5^+TCF1^+$ T_{PEX} cells. Results are representative of two or three
347 independent experiments (*n* = 4-5/group). Each dot represents one individual mouse.
348 Student's unpaired two-tailed t tests.

349

350 **Figure 2. IL-2 alters tissue localization of $CD8^+$ T cells and viral reservoirs in chronic**
351 **infection.**

352 (**A**) C57BL/6 mice were chronically infected with LCMV Docile and received
353 intraperitoneal treatment with IL-2 as in Figure 1A. Representative confocal images (left:
354 low magnification, right: high magnification) and quantification of LCMV infected cells in
355 the spleen. (**B**) C57BL/6 mice chronically infected with LCMV Docile and receiving
356 intraperitoneal treatment of gradient doses of recombinant human IL-2 (10,000 – 100,000
357 IU) daily from day 10 to 14 post infection, followed by the analyses on day 15. FACS plot
358 showing the gating of T_{FH} and non-T_{FH} cells in $CD4^+$ T cells (left), and quantification of
359 virus-infected ($VL4^+$) T_{FH} and non-T_{FH} cells in each group (right). (**C**, **D**) In the same
360 experiment as (A), histograms showing the expression of CXCR5 on GP_{33} tetramer-
361 specific $CXCR5^+$ $CD8^+$ T cells (C) and representative images (left) and quantification
362 (right) of $CD8^+$ T cells in B-cell follicles (D). (**E**) Representative FACS plots (left) and

363 quantification (right) showing the expression of CXCR5$^+$ on OT-I CD8$^+$ T cells, co-cultured
364 with splenocytes pulsed with the SINFEKL peptide (1 μM) and indicated cytokines: TGFβ
365 (10 ng/mL), IL-6 (100 ng/mL) and IL-2 (500 I.U./mL). Results are representative of at least
366 two independent experiments. Each dot represents one image count (A, D), one individual
367 mouse (B), or one culture (E). Student's unpaired two-tailed t tests.
368
369 **Figure 3. An IL-2-STAT5-BLIMP1 axis regulates the balance of effector and T_{PEX}**
370 **generation.**
371 (**A-C**) C57BL/6 mice were chronically infected with LCMV Docile and received
372 intraperitoneal treatment with IL-2 as in Figure 1A. Quantification of the expression of
373 CD122 and CD25 between CXCR5$^+$ T_{PEX} cells and CXCR5$^-$ T_{EX} cells (A). The comparison
374 of the expression of CD122 and CD25 on CXCR5$^+$ T_{PEX} cells or CXCR5$^-$ T_{EX} cells between
375 PBS treated and IL-2 treated mice (B). The comparison of the expression of pSTAT5 in
376 CXCR5$^+$ T_{PEX} cells or CXCR5$^-$ T_{EX} cells between PBS treated and IL-2 treated mice (C).
377 (**D-F**) Schematic (D) showing the overexpression of constitutive active STAT5b (STAT5b-
378 CA) in P14 cells, followed by the adoptive transfer in congenically marked recipient mice
379 with chronical LCMV Docile infection. Representative FACS plots (left) and quantifications
380 (right) of the frequencies of P14 cells in total CD8$^+$ T cells (E) and the frequencies of
381 CXCR5$^+$ T_{PEX} cells in P14 cells (F). (**G**, **H**) Schematic of the generation of bone marrow
382 chimera mice carrying T cell specific deletion of BLIMP1 (encoded by *Prdm1*), followed
383 with chronic LCMV Docile infection and IL-2 treatment (i.p. 30,000 I.U. daily from day 10
384 to 14 post-infection) (G). Representative FACS plots and quantifications showing the
385 frequencies of CXCR5$^+$ T_{PEX} cells in CD44$^+$ CD8$^+$ T cells (H). Results are representative
386 of two or three independent experiments (n = 4-5/group). Each dot represents one
387 individual mouse. Student's unpaired two-tailed t tests. N.S., statistically not significant.
388
389 **Figure 4. An IL-2 fusion protein regulates the balance of effector and T_{PEX} cell**
390 **generation.**
391 (**A**) Schematic showing P14 T cells being transferred into congenically marked mice,
392 which were subsequently infected with LCMV Docile and treated with ANV410, a CD122-
393 specific IL-2 fusion protein, three times every other day from day 8 to 12 post infection

394 and analyzed on day 14 post infection (regimen 1, panels B-E) or from day 1 to 5 of
395 infection and analyzed on day 7 post infection (regimen 2, panels F-H). (**B**)
396 Quantifications of total $CD8^+$ T cells (left) or P14 cells (right) on day 14 post infection
397 (regimen 1). (**C**) FACS plot showing the gating strategy for $CX3CR1^+$ T_{EX} cells (left) and
398 quantifications of percentages and numbers of $CX3CR1^+$ T_{EX} cells in P14 cells on day 14
399 post infection (regimen 1). (**D**) Quantification showing percentages and expression levels
400 of $GzmB^+$ P14 cells on day 14 post infection (regimen 1). (**E**) FACS plots showing the
401 gating strategy for $TCF1^+$ T_{PEX} cells (left) and quantification showing the percentages and
402 numbers of $TCF1^+$ T_{PEX} cells in P14 cells on day 14 post infection (regimen 1). (**F**)
403 Quantification showing the percentages and numbers of P14 cells on day 7 post infection
404 (regimen 2). (**G**) FACS plots showing the gating strategy for $TCF1^+$ T_{PEX} cells (left) and
405 quantification showing the percentages and numbers of $TCF1^+$ T_{PEX} cells in P14 cells on
406 day 7 post infection (regimen 2). (**H**) Quantification showing the percentages and
407 numbers of $TCF1^+$ T_{PEX} cells in endogenous PD-1^+ $CD8^+$ T cells on day 7 post infection
408 (regimen 2). (**I**) Schematic of low-dose IL-2 therapy in patients with systemic lupus
409 erythematosus (SLE). (**J**) Quantification showing the frequencies of $CXCR5^+$ T_{PEX} in
410 peripheral blood $CD8^+$ T cells in consecutive time points (left) or before and after the
411 therapy (right). Each dot represents one individual mouse (B-H) or one individual patient
412 (J). Student's unpaired two-tailed t tests (B-H) and paired two-tailed t test (J).
413
414
415
416
417
418
419
420
421
422
423
424

425

426

427 **STAR ★ METHODS**

428 **RESOURCE AVAILABILITY**

429 **Lead contact**

430 Further information and requests for resources and reagents should be directed to and
431 will be fulfilled by the lead contact, Di Yu (di.yu@uq.edu.au).

432

433 **Materials availability**

434 This study did not generate new unique reagents.

435 **Data and code availability**

436 RNA-seq data were generated from datasets publicly available at GEO. Accession
437 numbers are listed in the Key resources table. qPCR data, microscopy data, and any
438 additional information required to reanalyse the data reported in this paper are available
439 from the lead contact upon request. This paper does not report original code. Scripts and
440 code utilised in this study are available from the lead contact upon request. Information
441 regarding microglia isolation and sequencing can be addressed to Di Yu
442 (di.yu@uq.edu.au).

443

444 **EXPERIMENTAL MODEL AND STUDY PARTICIPANT DETAILS**

445

446 **Mice**

447 All mice used in this study were held in SPF (specific pathogen free) animal facilities in
448 The Australian National University, Monash University, University of Melbourne or the
449 Walter and Eliza Hall Institute (WEHI). 6-12 weeks C57BL/6 mice or *Ptprca* (CD45.1)
450 mice were used for *in vivo* and *in vitro* experiments. P14 mice (JAX Tg(TcrLCMV)327Sdz)
451 with the transgenic expression of a TCR specific for LCMV glycoprotein $(GP)_{33\text{-}41}$ were
452 used for adoptive transfer experiment, and OT-I mice are with the transgenic expression
453 of a TCR specific for chicken ovalbumin $(OVA)_{257\text{-}264}$. *Lck*^{Cre} mice *were crossed with*

454 *Prdm1*$^{flox/flox}$ mice (Kallies et al., 2009). All animal experiment ethics were approved by
455 the designated Animal Ethics Committee of the institutes that were responsible for animal
456 experiments.
457
458 **Human data**
459 The details of the prospective, open-label study of low-dose recombinant human IL-2
460 (rhIL-2) in patients with active SLE was described (He et al., 2016a). Briefly, three cycles
461 of rhIL-2 were administered subcutaneously at a dose of 1 million IU every other day for
462 2 weeks (a total of 7 doses), followed by a 2-week break. Immunological data in peripheral
463 blood mononuclear cells (PBMCs) were measured at baseline and every 2 weeks
464 thereafter until week 12.
465
466 **METHOD DETAILS**
467
468 **Viral infection**
469 Lymphocytic choriomeningitis virus (LCMV) Docile was propagated using BHK cell line
470 which was cultured with complete DMEM medium. To study the role of IL-2 treatment in
471 chronic LCMV infection, mice were intravenously (i.v.) infected with 1-2×10^6 PFU (plaque-
472 forming units) of LCMV Docile virus in 100 ul of PBS.
473
474 **IL-2 and ANV410 treatment**
475 10,000 to 100,000 I.U. (international units) of human rhIL-2 (recombinant human IL-
476 2^{Ser125}, Beijing SL Pharma) were intraperitoneally (i.p.) injected into the mice daily for 5
477 times from days 10 to 14 post LCMV Docile infection. Mice were sacrificed on day 15 post
478 infection and samples were collected for further examination. ANV410, supplied by
479 Anaveon AG (Basel, Switzerland), is a human IL-2/anti-IL-2 circularly permutated fusion
480 protein which selectively signals through the intermediate affinity IL-2R (IL-2Rβ/γ). For
481 treatment with ANV410, naïve or Docile infected mice were treated with 200 μg/kg body
482 weight three times (every other day in five days).
483
484 **Generation of bone marrow chimeric mice**

485 Bone marrow (BM) cells were collected from femurs of 6-12 weeks old mice with indicated
486 genotypes. Single cells were prepared by pipetting in complete RPMI media. CD45.1
487 recipient mouse were lethally irradiated twice with 4.75 gray (Gy) of gamma radiation 4
488 hours apart. BLIMP1-deficient BM cells (CD45.2) were mixed with wildtype control BM
489 cells (CD45.1/CD45.2) at 1:1 ratio and intravenously transferred into irradiated CD45.1
490 recipient mouse. As control, BM cells from genotyped wild type littermates (CD45.2) were
491 also mixed with wildtype control BM (CD45.1/CD45.2) and reconstituted in recipient
492 CD45.1 mice. Mice were housed for 6 to 8 weeks to allow hematopoietic reconstitution
493 before infection with LCMV Docile virus.
494
495 ***In vitro* induction of CXCR5$^+$ CD8$^+$ cells**
496 For induction of CXCR5$^+$ CD8$^+$ T cells, naïve OT-I cells (CD8$^+$Va2$^+$CD44$^-$CD62L$^+$) were
497 purified (10^4 cells/well) and co-cultured with congenical wildtype splenocytes (10^5
498 cells/well) in 96-well plates, in the presence of the SINFEKL peptide (1 μM) with indicated
499 cytokines: TGFβ (10 ng/mL), IL-6 (100 ng/mL) and IL-2 (500 I.U./mL~30-50ng/mL).
500
501 **Retroviral transduction on primary cells**
502 GFP bicistronic retroviral vector containing STAT5b-CA or empty vector as described
503 (Johnston et al., 2012) were used to study the overexpression of STAT5b-CA in primary
504 mouse CD8$^+$ T cells. Retroviruses were generated by transfecting the plasmids into a
505 retrovirus-packaging cell line GPE86 using lipofectamine 2000 reagent (Invitrogen). GFP
506 positive GPE86 were cell sorted to isolate stably transfected cells. Stably transfected
507 GPE86 were then cultured in complete DMEM media for 48 hours before the culture
508 supernatant were collected for the transduction of primary cells. Naïve P14 T cells were
509 purified from CD45.2 TCR transgenic P14 mice and stimulated with plate bound anti-CD3
510 and anti-CD28 for 48 hours. Activated P14 T cells were spinoculated at 800g for 1 hour
511 at 32°C with the retrovirus supernatants packaged by GPE86 cells. Transduced P14 T
512 cells were rested in fresh cRPMI media containing 20 ng/mL of rmIL-7 for 48 hours. About
513 6,000 GFP$^+$ P14 T cells were sorted by flow cytometry and intravenously (i.v.) transferred
514 into CD45.1 recipient mouse. One day after adoptive transfer, mice were i.v. infected with
515 LCMV Docile at 10^6 PFU. Mice were culled on day 8 post infection for analyses.

516

517 **Flow cytometry**

518 Single cells were washed, counted, and stained with Fc-receptor blocking antibodies
519 (clone 2.4G2, 1:100 dilution, BD) for 10 min on ice to block non-specific staining. For
520 surface staining, cells were washed once with PBS containing 2% heat-inactivated fetal
521 bovine serum (FBS, Gibco) and stained in an appropriately diluted antibody solution for
522 at least 30 min at 4 °C. The 7-amino-actinomycin D (7-AAD) (BioLegend) was stained to
523 exclude dead cells. For intracellular staining, Cytofix/Cytoperm (BD) was used as user's
524 guide. For intranuclear staining, Foxp3/Transcription Factor Staining Buffer Set
525 (eBioscience) was used as user's guide. To detect LCMV antigen-specific $CD8^+$ T cells,
526 APC-conjugated H-$2D^b$-GP_{33}-tetramer (produced by Biomolecular Resource Facility at
527 The John Curtin School of Medical Research, The Australian National University). To
528 detect LCMV-infected T cells, purified anti-LCMV nucleoprotein (clone VL4) antibody was
529 labelled with Alexa Fluor (AF) 647 using antibody labelling kit (Invitrogen). Splenocytes
530 from LCMV infected mice were first stained with surface antibodies. After permeabilization
531 by the Cytofix/Cytoperm (BD) kit, labelled AF647-VL4 antibody was incubated with the
532 cells for 30 min at 25 °C. Uninfected splenocytes and VL4 unstained splenocytes were
533 used as negative control. Data were collected on a LSR-II or LSRFortessaTM (BD) and
534 analyzed using FlowJo software.

535

536 **Immunofluorescence**

537 To visualize LCMV infection and P14 cells in splenic tissues, immunofluorescent staining
538 was performed. The middle section of spleens was cut and submerged immediately in
539 Optimal Cutting Temperature (OCT) compound on dry ice and stored at -80°C. OCT
540 blocks were then sectioned at 5 to 10 μm thickness at -20°C. Sections were blocked with
541 Fc-receptor-blocking antibody (clone 2.4G2, 1:100, BD), followed by staining with primary
542 antibodies. Then sections were washed and stained with secondary antibodies or
543 streptavidin. All steps were performed at 25 °C for 60 min in dark and sections were
544 mounted using Prolong Gold (Invitrogen). Slides were visualized using laser scanning
545 confocal microscopy (Leica SP5) at the John Curtin School of Medical Research.

546 Quantification of infected cells was performed by automatic counting of cells per area of
547 section using Imaris 9.0 software.
548
549 **RNA sequencing and bioinformatics analysis**

550 RNA sequencing and bioinformatic analyses to compare the transcriptomes between
551 CXCR5^{-} and CXCR5^{+} P14 cells were described previously (Leong et al., 2016). DESeq2
552 from Bioconductor software (Love et al., 2014) was used to normalize gene counts in
553 GSE76279 dataset, and the genes were ranked based on -log(adjusted p-value of fold
554 change). The ranked list was introduced to GSEA software (Subramanian et al., 2005) to
555 enrich genes in gene sets of a wide range of databases using a curated version of "msigdb
556 v7.2 symbols". The normalized counts were also filtered for interleukin receptors to
557 produce a heatmap using pheatmap function in r and to construct a bar chart in GraphPad
558 Prism 9. Multiple unpaired t-tests were used to show the level of significancy.
559
560 **QUANTIFICATION AND STATISTICAL ANALYSIS**
561
562 **Statistical analysis**
563 All results were analyzed by unpaired or paired and two-tailed student t-test for
564 comparison between two groups or one-way ANOVA for calculating univariate data set
565 with more than two groups by GraphPad Prism 8.0 software, unless otherwise specified.
566 Differences were considered to be statistically significant at $p < 0.05$.
567
568
569
570

571 **Supplementary Materials**

572 **Fig. S1-S2.**

573 **References**

574 Alfei, F., Kanev, K., Hofmann, M., Wu, M., Ghoneim, H.E., Roelli, P., Utzschneider, D.T.,
575 von Hoesslin, M., Cullen, J.G., Fan, Y., et al. (2019). TOX reinforces the phenotype and
576 longevity of exhausted T cells in chronic viral infection. Nature 571, 265-269.

577 Beltra, J.C., Abdel-Hakeem, M.S., Manne, S., Zhang, Z., Huang, H., Kurachi, M., Su, L.,
578 Picton, L., Ngiow, S.F., Muroyama, Y., et al. (2023). Stat5 opposes the transcription factor
579 Tox and rewires exhausted CD8(+) T cells toward durable effector-like states during
580 chronic antigen exposure. Immunity 56, 2699-2718 e2611.

581 Beltra, J.C., Bourbonnais, S., Bedard, N., Charpentier, T., Boulange, M., Michaud, E.,
582 Boufaied, I., Bruneau, J., Shoukry, N.H., Lamarre, A., et al. (2016). IL2Rbeta-dependent
583 signals drive terminal exhaustion and suppress memory development during chronic viral
584 infection. Proc Natl Acad Sci U S A 113, E5444-5453.

585 Blank, C.U., Haining, W.N., Held, W., Hogan, P.G., Kallies, A., Lugli, E., Lynn, R.C., Philip,
586 M., Rao, A., Restifo, N.P., et al. (2019). Defining 'T cell exhaustion'. Nat Rev Immunol 19,
587 665-674.

588 Blattman, J.N., Grayson, J.M., Wherry, E.J., Kaech, S.M., Smith, K.A., and Ahmed, R.
589 (2003). Therapeutic use of IL-2 to enhance antiviral T-cell responses in vivo. Nat Med 9,
590 540-547.

591 Boyman, O., and Sprent, J. (2012). The role of interleukin-2 during homeostasis and
592 activation of the immune system. Nat Rev Immunol 12, 180-190.

593 Codarri Deak, L., Nicolini, V., Hashimoto, M., Karagianni, M., Schwalie, P.C., Lauener,
594 L., Varypataki, E.M., Richard, M., Bommer, E., Sam, J., et al. (2022). PD-1-cis IL-2R
595 agonism yields better effectors from stem-like CD8(+) T cells. Nature 610, 161-172.

596 Collins, D.R., Hitschfel, J., Urbach, J.M., Mylvaganam, G.H., Ly, N.L., Arshad, U.,
597 Racenet, Z.J., Yanez, A.G., Diefenbach, T.J., and Walker, B.D. (2023). Cytolytic CD8(+)
598 T cells infiltrate germinal centers to limit ongoing HIV replication in spontaneous controller
599 lymph nodes. Sci Immunol 8, eade5872.

600 Dutcher, J.P., Schwartzentruber, D.J., Kaufman, H.L., Agarwala, S.S., Tarhini, A.A.,
601 Lowder, J.N., and Atkins, M.B. (2014). High dose interleukin-2 (Aldesleukin) - expert
602 consensus on best management practices-2014. J Immunother Cancer 2, 26.

603 Eberhardt, C.S., Kissick, H.T., Patel, M.R., Cardenas, M.A., Prokhnevska, N., Obeng,
604 R.C., Nasti, T.H., Griffith, C.C., Im, S.J., Wang, X., et al. (2021). Functional HPV-specific
605 PD-1(+) stem-like CD8 T cells in head and neck cancer. Nature 597, 279-284.

606 Gabriel, S.S., Tsui, C., Chisanga, D., Weber, F., Llano-Leon, M., Gubser, P.M., Bartholin,
607 L., Souza-Fonseca-Guimaraes, F., Huntington, N.D., Shi, W., et al. (2021). Transforming
608 growth factor-beta-regulated mTOR activity preserves cellular metabolism to maintain
609 long-term T cell responses in chronic infection. Immunity 54, 1698-1714 e1695.

610 Gautam, S., Fioravanti, J., Zhu, W., Le Gall, J.B., Brohawn, P., Lacey, N.E., Hu, J.,
611 Hocker, J.D., Hawk, N.V., Kapoor, V., et al. (2019). The transcription factor c-Myb
612 regulates CD8(+) T cell stemness and antitumor immunity. Nat Immunol 20, 337-349.

613 Hashimoto, M., Araki, K., Cardenas, M.A., Li, P., Jadhav, R.R., Kissick, H.T., Hudson,
614 W.H., McGuire, D.J., Obeng, R.C., Wieland, A., et al. (2022). PD-1 combination therapy
615 with IL-2 modifies CD8(+) T cell exhaustion program. Nature 610, 173-181.

616 Hashimoto, M., Kamphorst, A.O., Im, S.J., Kissick, H.T., Pillai, R.N., Ramalingam, S.S.,
617 Araki, K., and Ahmed, R. (2018). CD8 T Cell Exhaustion in Chronic Infection and Cancer:
618 Opportunities for Interventions. Annu Rev Med 69, 301-318.

619 He, J., Zhang, X., Wei, Y., Sun, X., Chen, Y., Deng, J., Jin, Y., Gan, Y., Hu, X., Jia, R., et
620 al. (2016a). Low-dose interleukin-2 treatment selectively modulates CD4(+) T cell subsets
621 in patients with systemic lupus erythematosus. Nat Med 22, 991-993.

622 He, R., Hou, S., Liu, C., Zhang, A., Bai, Q., Han, M., Yang, Y., Wei, G., Shen, T., Yang,
623 X., et al. (2016b). Follicular CXCR5- expressing CD8(+) T cells curtail chronic viral
624 infection. Nature 537, 412-428.

625 Hu, Y., Hudson, W.H., Kissick, H.T., Medina, C.B., Baptista, A.P., Ma, C., Liao, W.,
626 Germain, R.N., Turley, S.J., Zhang, N., et al. (2022). TGF-beta regulates the stem-like
627 state of PD-1+ TCF-1+ virus-specific CD8 T cells during chronic infection. J Exp Med 219.

628 Huang, Q., Wu, X., Wang, Z., Chen, X., Wang, L., Lu, Y., Xiong, D., Liu, Q., Tian, Y., Lin,
629 H., et al. (2022). The primordial differentiation of tumor-specific memory CD8(+) T cells
630 as bona fide responders to PD-1/PD-L1 blockade in draining lymph nodes. Cell 185,
631 4049-4066 e4025.

632 Hudson, W.H., Gensheimer, J., Hashimoto, M., Wieland, A., Valanparambil, R.M., Li, P.,
633 Lin, J.X., Konieczny, B.T., Im, S.J., Freeman, G.J., et al. (2019). Proliferating Transitory
634 T Cells with an Effector-like Transcriptional Signature Emerge from PD-1(+) Stem-like
635 CD8(+) T Cells during Chronic Infection. Immunity 51, 1043-1058 e1044.

636 Humblet-Baron, S., Franckaert, D., Dooley, J., Bornschein, S., Cauwe, B., Schonefeldt,
637 S., Bossuyt, X., Matthys, P., Baron, F., Wouters, C., et al. (2016). IL-2 consumption by
638 highly activated CD8 T cells induces regulatory T-cell dysfunction in patients with
639 hemophagocytic lymphohistiocytosis. J Allergy Clin Immunol 138, 200-209 e208.

640 Im, S.J., Hashimoto, M., Gerner, M.Y., Lee, J., Kissick, H.T., Burger, M.C., Shan, Q.,
641 Hale, J.S., Lee, J., Nasti, T.H., et al. (2016). Defining CD8+ T cells that provide the
642 proliferative burst after PD-1 therapy. Nature 537, 417-421.

643 Johnston, R.J., Choi, Y.S., Diamond, J.A., Yang, J.A., and Crotty, S. (2012). STAT5 is a
644 potent negative regulator of TFH cell differentiation. J Exp Med 209, 243-250.

645 Johnston, R.J., Poholek, A.C., DiToro, D., Yusuf, I., Eto, D., Barnett, B., Dent, A.L., Craft,
646 J., and Crotty, S. (2009). Bcl6 and Blimp-1 are reciprocal and antagonistic regulators of
647 T follicular helper cell differentiation. Science 325, 1006-1010.

648 Kallies, A., Xin, A., Belz, G.T., and Nutt, S.L. (2009). Blimp-1 transcription factor is
649 required for the differentiation of effector CD8+ T cells and memory responses. Immunity
650 31, 283-295.

651 Kallies, A., Zehn, D., and Utzschneider, D.T. (2020). Precursor exhausted T cells: key to
652 successful immunotherapy? Nat Rev Immunol 20, 128-136.

653 Khan, O., Giles, J.R., McDonald, S., Manne, S., Ngiow, S.F., Patel, K.P., Werner, M.T.,
654 Huang, A.C., Alexander, K.A., Wu, J.E., et al. (2019). TOX transcriptionally and
655 epigenetically programs CD8(+) T cell exhaustion. Nature 571, 211-218.

656 Kunz, S., Sevilla, N., McGavern, D.B., Campbell, K.P., and Oldstone, M.B. (2001).
657 Molecular analysis of the interaction of LCMV with its cellular receptor [alpha]-
658 dystroglycan. J Cell Biol 155, 301-310.

659 Leong, Y.A., Chen, Y., Ong, H.S., Wu, D., Man, K., Deleage, C., Minnich, M., Meckiff,
660 B.J., Wei, Y., Hou, Z., et al. (2016). CXCR5(+) follicular cytotoxic T cells control viral
661 infection in B cell follicles. Nat Immunol 17, 1187-1196.

662 Liu, Y., Zhou, N., Zhou, L., Wang, J., Zhou, Y., Zhang, T., Fang, Y., Deng, J., Gao, Y.,
663 Liang, X., et al. (2021). IL-2 regulates tumor-reactive CD8(+) T cell exhaustion by
664 activating the aryl hydrocarbon receptor. Nat Immunol 22, 358-369.

665 Love, M.I., Huber, W., and Anders, S. (2014). Moderated estimation of fold change and
666 dispersion for RNA-seq data with DESeq2. Genome Biol 15, 550.

667 Ma, C., Wang, L., Liao, W., Liu, Y., Mishra, S., Li, G., Zhang, X., Qiu, Y., Lu, Q., and
668 Zhang, N. (2022). TGF-beta promotes stem-like T cells via enforcing their lymphoid tissue
669 retention. J Exp Med 219.

670 Man, K., Gabriel, S.S., Liao, Y., Gloury, R., Preston, S., Henstridge, D.C., Pellegrini, M.,
671 Zehn, D., Berberich-Siebelt, F., Febbraio, M.A., et al. (2017). Transcription Factor IRF4
672 Promotes CD8(+) T Cell Exhaustion and Limits the Development of Memory-like T Cells
673 during Chronic Infection. Immunity 47, 1129-1141 e1125.

674 Martinez, G.J., Pereira, R.M., Aijo, T., Kim, E.Y., Marangoni, F., Pipkin, M.E., Togher, S.,
675 Heissmeyer, V., Zhang, Y.C., Crotty, S., et al. (2015). The transcription factor NFAT
676 promotes exhaustion of activated CD8(+) T cells. Immunity 42, 265-278.

677 Marx, A.F., Kallert, S.M., Brunner, T.M., Villegas, J.A., Geier, F., Fixemer, J., Abreu-Mota,
678 T., Reuther, P., Bonilla, W.V., Fadejeva, J., et al. (2023). The alarmin interleukin-33
679 promotes the expansion and preserves the stemness of Tcf-1(+) CD8(+) T cells in chronic
680 viral infection. Immunity 56, 813-828 e810.

681 McLane, L.M., Abdel-Hakeem, M.S., and Wherry, E.J. (2019). CD8 T Cell Exhaustion
682 During Chronic Viral Infection and Cancer. Annu Rev Immunol 37, 457-495.

683 Mylvaganam, G.H., Rios, D., Abdelaal, H.M., Iyer, S., Tharp, G., Mavigner, M., Hicks, S.,
684 Chahroudi, A., Ahmed, R., Bosinger, S.E., et al. (2017). Dynamics of SIV-specific

685 CXCR5+ CD8 T cells during chronic SIV infection. Proc Natl Acad Sci U S A 114, 1976-
686 1981.

687 Oldstone, M.B., and Campbell, K.P. (2011). Decoding arenavirus pathogenesis: essential
688 roles for alpha-dystroglycan-virus interactions and the immune response. Virology 411,
689 170-179.

690 Petrovas, C., Ferrando-Martinez, S., Gerner, M.Y., Casazza, J.P., Pegu, A., Deleage, C.,
691 Cooper, A., Hataye, J., Andrews, S., Ambrozak, D., et al. (2017). Follicular CD8 T cells
692 accumulate in HIV infection and can kill infected cells in vitro via bispecific antibodies. Sci
693 Transl Med 9.

694 Ren, Z., Zhang, A., Sun, Z., Liang, Y., Ye, J., Qiao, J., Li, B., and Fu, Y.X. (2022).
695 Selective delivery of low-affinity IL-2 to PD-1+ T cells rejuvenates antitumor immunity with
696 reduced toxicity. J Clin Invest 132.

697 Scott, A.C., Dundar, F., Zumbo, P., Chandran, S.S., Klebanoff, C.A., Shakiba, M., Trivedi,
698 P., Menocal, L., Appleby, H., Camara, S., et al. (2019). TOX is a critical regulator of
699 tumour-specific T cell differentiation. Nature 571, 270-274.

700 Seo, H., Chen, J., Gonzalez-Avalos, E., Samaniego-Castruita, D., Das, A., Wang, Y.H.,
701 Lopez-Moyado, I.F., Georges, R.O., Zhang, W., Onodera, A., et al. (2019). TOX and
702 TOX2 transcription factors cooperate with NR4A transcription factors to impose CD8(+)
703 T cell exhaustion. Proc Natl Acad Sci U S A 116, 12410-12415.

704 Siddiqui, I., Schaeuble, K., Chennupati, V., Fuertes Marraco, S.A., Calderon-Copete, S.,
705 Pais Ferreira, D., Carmona, S.J., Scarpellino, L., Gfeller, D., Pradervand, S., et al. (2019).
706 Intratumoral Tcf1(+)PD-1(+)CD8(+) T Cells with Stem-like Properties Promote Tumor
707 Control in Response to Vaccination and Checkpoint Blockade Immunotherapy. Immunity
708 50, 195-211 e110.

709 Subramanian, A., Tamayo, P., Mootha, V.K., Mukherjee, S., Ebert, B.L., Gillette, M.A.,
710 Paulovich, A., Pomeroy, S.L., Golub, T.R., Lander, E.S., et al. (2005). Gene set
711 enrichment analysis: a knowledge-based approach for interpreting genome-wide
712 expression profiles. Proc Natl Acad Sci U S A 102, 15545-15550.

713 Sun, Q., Cai, D., Liu, D., Zhao, X., Li, R., Xu, W., Xie, B., Gou, M., Wei, K., Li, Y., et al.
714 (2023). BCL6 promotes a stem-like CD8(+) T cell program in cancer via antagonizing
715 BLIMP1. Sci Immunol 8, eadh1306.

716 Tichet, M., Wullschleger, S., Chryplewicz, A., Fournier, N., Marcone, R., Kauzlaric, A.,
717 Homicsko, K., Deak, L.C., Umana, P., Klein, C., et al. (2023). Bispecific PD1-IL2v and
718 anti-PD-L1 break tumor immunity resistance by enhancing stem-like tumor-reactive
719 CD8(+) T cells and reprogramming macrophages. Immunity 56, 162-179 e166.

720 Tsui, C., Kretschmer, L., Rapelius, S., Gabriel, S.S., Chisanga, D., Knopper, K.,
721 Utzschneider, D.T., Nussing, S., Liao, Y., Mason, T., et al. (2022). MYB orchestrates T
722 cell exhaustion and response to checkpoint inhibition. Nature 609, 354-360.

723 Utzschneider, D.T., Charmoy, M., Chennupati, V., Pousse, L., Ferreira, D.P., Calderon-
724 Copete, S., Danilo, M., Alfei, F., Hofmann, M., Wieland, D., et al. (2016). T Cell Factor 1-
725 Expressing Memory-like CD8(+) T Cells Sustain the Immune Response to Chronic Viral
726 Infections. Immunity 45, 415-427.

727 Vinuesa, C.G., Linterman, M.A., Yu, D., and MacLennan, I.C. (2016). Follicular Helper T
728 Cells. Annu Rev Immunol 34, 335-368.

729 West, E.E., Jin, H.T., Rasheed, A.U., Penaloza-Macmaster, P., Ha, S.J., Tan, W.G.,
730 Youngblood, B., Freeman, G.J., Smith, K.A., and Ahmed, R. (2013). PD-L1 blockade
731 synergizes with IL-2 therapy in reinvigorating exhausted T cells. J Clin Invest 123, 2604-
732 2615.

733 Wu, T., Ji, Y., Moseman, E.A., Xu, H.C., Manglani, M., Kirby, M., Anderson, S.M.,
734 Handon, R., Kenyon, E., Elkahloun, A., et al. (2016). The TCF1-Bcl6 axis counteracts
735 type I interferon to repress exhaustion and maintain T cell stemness. Sci Immunol 1.

736 Xin, A., Masson, F., Liao, Y., Preston, S., Guan, T., Gloury, R., Olshansky, M., Lin, J.X.,
737 Li, P., Speed, T.P., et al. (2016). A molecular threshold for effector CD8(+) T cell
738 differentiation controlled by transcription factors Blimp-1 and T-bet. Nat Immunol 17, 422-
739 432.

740 Yan, Y., Cao, S., Liu, X., Harrington, S.M., Bindeman, W.E., Adjei, A.A., Jang, J.S., Jen,
741 J., Li, Y., Chanana, P., et al. (2018). CX3CR1 identifies PD-1 therapy-responsive CD8+
742 T cells that withstand chemotherapy during cancer chemoimmunotherapy. JCI Insight 3.

743 Yao, C., Sun, H.W., Lacey, N.E., Ji, Y., Moseman, E.A., Shih, H.Y., Heuston, E.F., Kirby,
744 M., Anderson, S., Cheng, J., et al. (2019). Single-cell RNA-seq reveals TOX as a key
745 regulator of CD8(+) T cell persistence in chronic infection. Nat Immunol 20, 890-901.

746 Yu, D., Walker, L.S.K., Liu, Z., Linterman, M.A., and Li, Z. (2022). Targeting T(FH) cells
747 in human diseases and vaccination: rationale and practice. Nat Immunol 23, 1157-1168.

748 Yu, D., and Ye, L. (2018). A Portrait of CXCR5(+) Follicular Cytotoxic CD8(+) T cells.
749 Trends Immunol 39, 965-979.

750 Zander, R., Kasmani, M.Y., Chen, Y., Topchyan, P., Shen, J., Zheng, S., Burns, R.,
751 Ingram, J., Cui, C., Joshi, N., et al. (2022). Tfh-cell-derived interleukin 21 sustains effector
752 CD8(+) T cell responses during chronic viral infection. Immunity 55, 475-493 e475.

753 Zander, R., Schauder, D., Xin, G., Nguyen, C., Wu, X., Zajac, A., and Cui, W. (2019).
754 CD4(+) T Cell Help Is Required for the Formation of a Cytolytic CD8(+) T Cell Subset that
755 Protects against Chronic Infection and Cancer. Immunity 51, 1028-1042 e1024.

756 Zhou, P., Chen, J., He, J., Zheng, T., Yunis, J., Makota, V., Alexandre, Y.O., Gong, F.,
757 Zhang, X., Xie, W., et al. (2021). Low-dose IL-2 therapy invigorates CD8+ T cells for viral
758 control in systemic lupus erythematosus. PLoS Pathog 17, e1009858.

759

760

Figure 1.

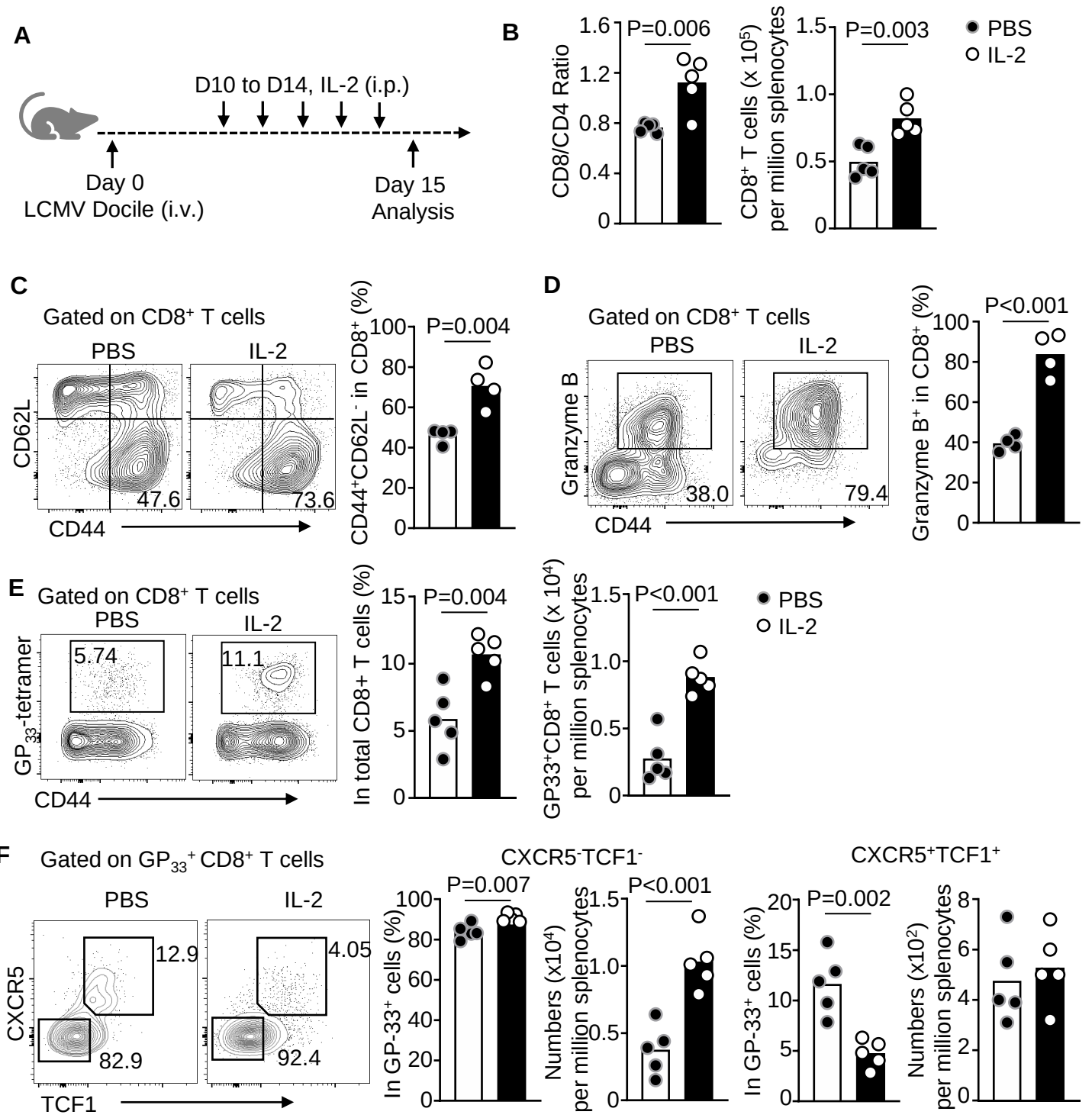
A
D10 to D14, IL-2 (i.p.)
Day 0
LCMV Docile (i.v.)
Day 15
Analysis
B
CD8/CD4 Ratio
P=0.006
CD8+ T cells (x 10^5) per million splenocytes
P=0.003
PBS
IL-2
C
Gated on CD8+ T cells
PBS
IL-2
CD62L
CD44
47.6
73.6
CD44+CD62L- in CD8+ (%)
P=0.004
D
Gated on CD8+ T cells
PBS
IL-2
Granzyme B
CD44
38.0
79.4
Granzyme B+ in CD8+ (%)
P<0.001
E
Gated on CD8+ T cells
PBS
IL-2
GP33-tetramer
CD44
5.74
11.1
In total CD8+ T cells (%)
P=0.004
GP33+CD8+ T cells (x 10^4) per million splenocytes
P<0.001
PBS
IL-2
F
Gated on GP33+ CD8+ T cells
PBS
IL-2
CXCR5
TCF1
12.9
82.9
4.05
92.4
CXCR5-TCF1-
In GP-33+ cells (%)
P=0.007
Numbers (x10^4) per million splenocytes
P<0.001
CXCR5+TCF1+
In GP-33+ cells (%)
P=0.002
Numbers (x10^2) per million splenocytes

Figure 2.

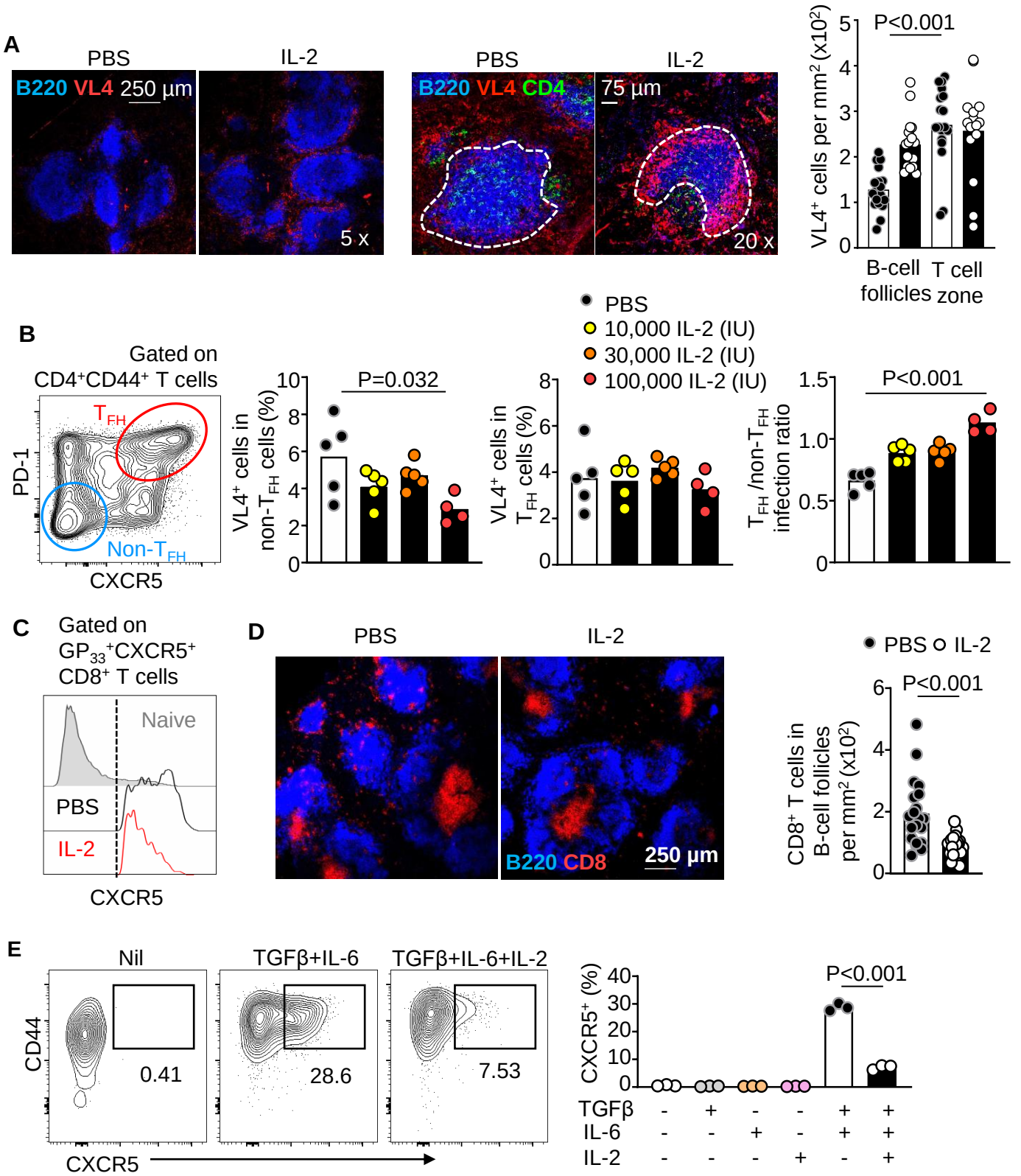
A
PBS
IL-2
B220 VL4 250 µm
5 x
PBS
IL-2
B220 VL4 CD4
75 µm
20 x
VL4+ cells per mm2 (x10^2)
P<0.001
B-cell follicles
T cell zone
B
Gated on CD4+CD44+ T cells
TFH
Non-TFH
PD-1
CXCR5
VL4+ cells in non-TFH cells (%)
P=0.032
PBS
10,000 IL-2 (IU)
30,000 IL-2 (IU)
100,000 IL-2 (IU)
VL4+ cells in TFH cells (%)
TFH /non-TFH infection ratio
P<0.001
C
Gated on GP33+CXCR5+ CD8+ T cells
Naive
PBS
IL-2
CXCR5
D
PBS
IL-2
B220 CD8
250 µm
PBS IL-2
P<0.001
CD8+ T cells in B-cell follicles per mm2 (x10^2)
E
Nil
TGFβ+IL-6
TGFβ+IL-6+IL-2
CD44
0.41
28.6
7.53
CXCR5
CXCR5+ (%)
P<0.001
TGFβ - + - - + +
IL-6 - - + - + +
IL-2 - - - + - +

Figure 3.

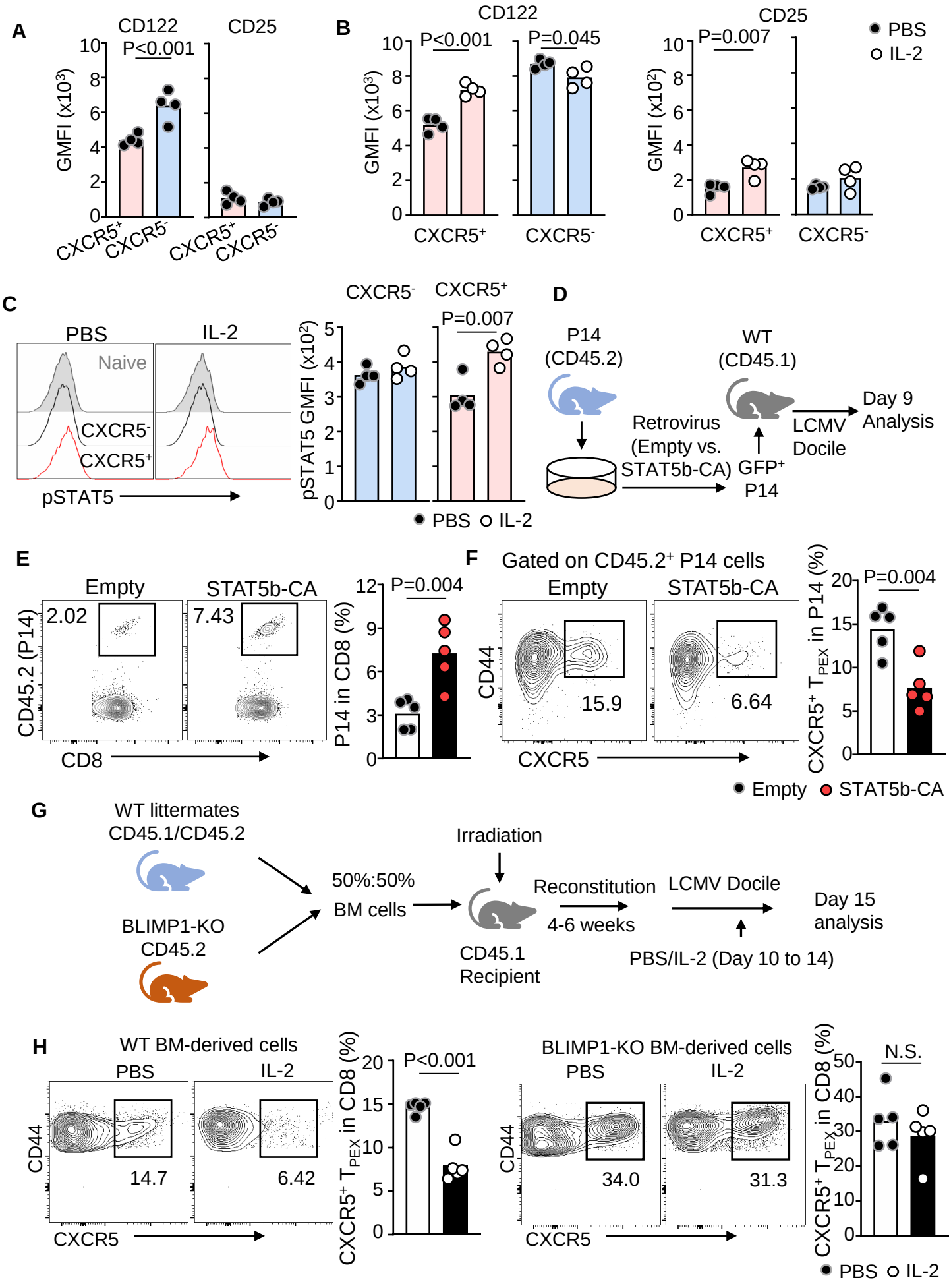
A
CD122
CD25
P<0.001
GMFI (x10³)
CXCR5⁺
CXCR5⁻
B
CD122
CD25
P<0.001
P=0.045
P=0.007
GMFI (x10³)
GMFI (x10²)
PBS
IL-2
C
PBS
IL-2
Naive
CXCR5⁻
CXCR5⁺
pSTAT5
pSTAT5 GMFI (x10²)
P=0.007
D
P14
(CD45.2)
WT
(CD45.1)
Retrovirus
(Empty vs.
STAT5b-CA)
GFP⁺
P14
LCMV
Docile
Day 9
Analysis
E
Empty
STAT5b-CA
2.02
7.43
CD45.2 (P14)
CD8
P14 in CD8 (%)
P=0.004
F
Gated on CD45.2⁺ P14 cells
Empty
STAT5b-CA
CD44
CXCR5
15.9
6.64
CXCR5⁺ T_PEX in P14 (%)
P=0.004
Empty
STAT5b-CA
G
WT littermates
CD45.1/CD45.2
BLIMP1-KO
CD45.2
50%:50%
BM cells
Irradiation
CD45.1
Recipient
Reconstitution
4-6 weeks
LCMV Docile
PBS/IL-2 (Day 10 to 14)
Day 15
analysis
H
WT BM-derived cells
PBS
IL-2
CD44
CXCR5
14.7
6.42
CXCR5⁺ T_PEX in CD8 (%)
P<0.001
BLIMP1-KO BM-derived cells
PBS
IL-2
34.0
31.3
N.S.
PBS
IL-2

Figure 4.

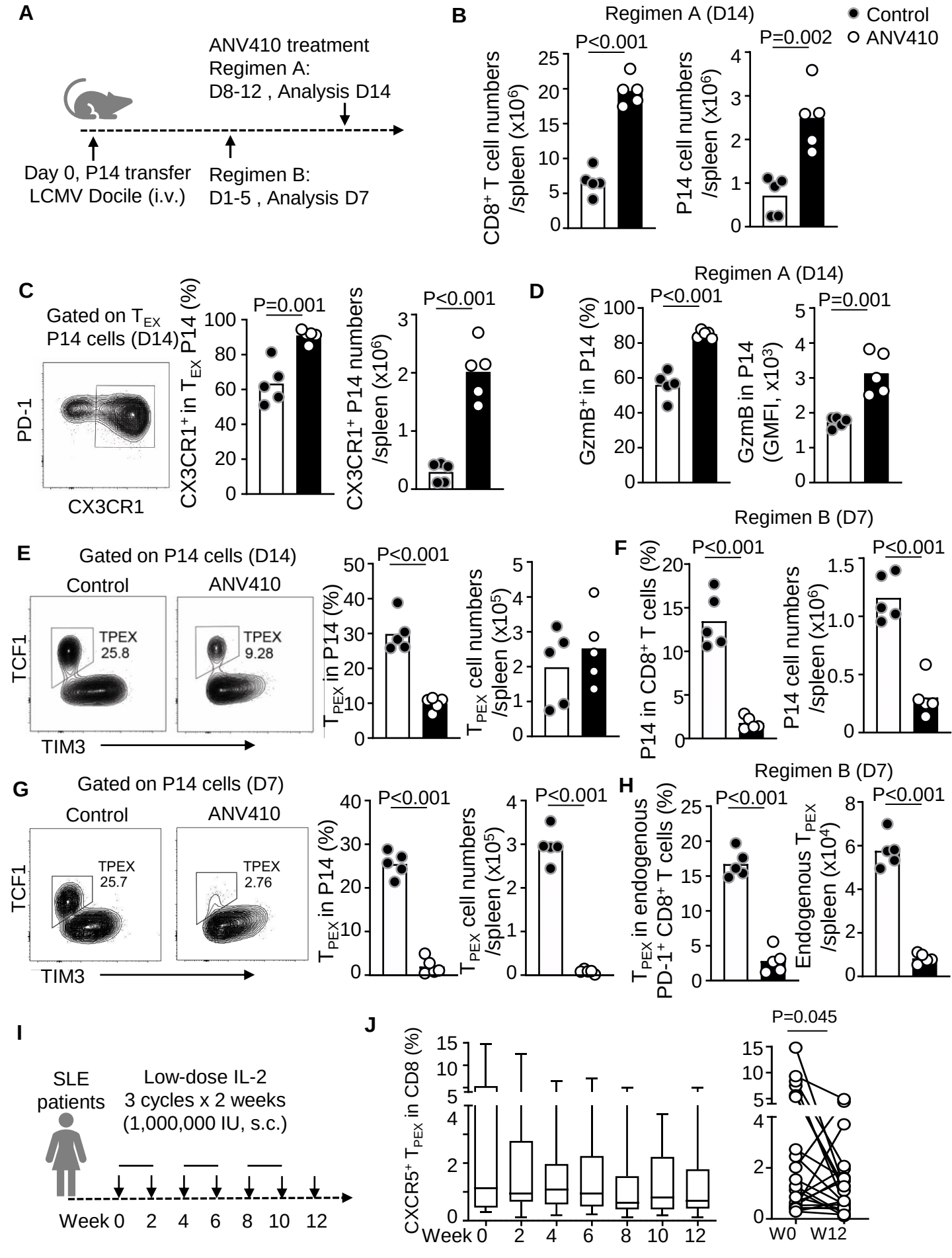
A
ANV410 treatment
Regimen A:
D8-12 , Analysis D14
Day 0, P14 transfer
LCMV Docile (i.v.)
Regimen B:
D1-5 , Analysis D7
B
Regimen A (D14)
Control
ANV410
P<0.001
P=0.002
CD8+ T cell numbers /spleen (x10^6)
P14 cell numbers /spleen (x10^6)
C
Gated on TEX P14 cells (D14)
PD-1
CX3CR1
P=0.001
P<0.001
CX3CR1+ in TEX P14 (%)
CX3CR1+ P14 numbers /spleen (x10^6)
D
Regimen A (D14)
P<0.001
P=0.001
GzmB+ in P14 (%)
GzmB in P14 (GMFI, x10^3)
E
Gated on P14 cells (D14)
Control
ANV410
TCF1
TIM3
TPEX 25.8
TPEX 9.28
P<0.001
TPEX in P14 (%)
TPEX cell numbers /spleen (x10^5)
F
Regimen B (D7)
P<0.001
P<0.001
P14 in CD8+ T cells (%)
P14 cell numbers /spleen (x10^6)
G
Gated on P14 cells (D7)
Control
ANV410
TCF1
TIM3
TPEX 25.7
TPEX 2.76
P<0.001
P<0.001
TPEX in P14 (%)
TPEX cell numbers /spleen (x10^5)
H
Regimen B (D7)
P<0.001
P<0.001
TPEX in endogenous PD-1+ CD8+ T cells (%)
Endogenous TPEX /spleen (x10^4)
I
SLE patients
Low-dose IL-2
3 cycles x 2 weeks
(1,000,000 IU, s.c.)
Week 0 2 4 6 8 10 12
J
P=0.045
CXCR5+ TPEX in CD8 (%)
Week 0 2 4 6 8 10 12
W0 W12

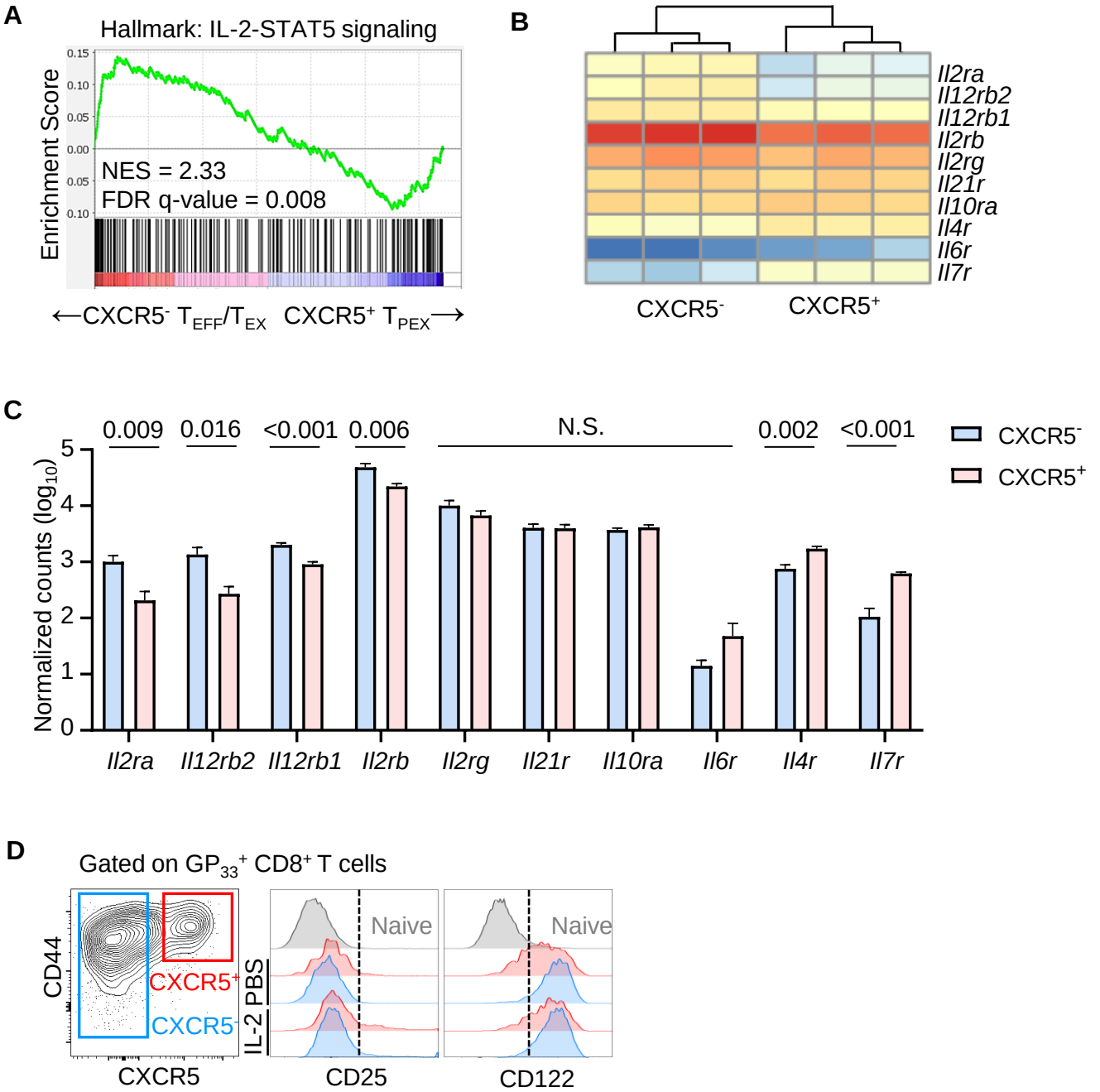

Suppl. Figure 1. Comparison of IL-2-STAT5 signaling and IL-2 receptors between CXCR5⁺ T_{PEX} cells and CXCR5⁻ T_{EX} cells.

(**A-C**) Purified CXCR5⁺ T_{PEX} and CXCR5⁻ T_{EX} P14 cells from host C57BL/6 mice at day 8 post LCMV (DOCILE) infection underwent RNA-seq to generate transcriptomes as described previously (Leong et al., 2016). Gene set enrichment analyses showing the downregulation of IL-2-STAT5 signalling in CXCR5+ T_{PEX} cells (A). Heatmaps (B) and quantification (C) showing the expression of indicated cytokine receptor genes.

(**D**) C57BL/6 mice were chronically infected with LCMV Docile and receiving intraperitoneal treatment of IL-2 as in Figure 1A. FACS plots showing the gating of CXCR5⁺ T_{PEX} cells and CXCR5⁻ T_{EX} populations in LCMV-specific GP_{33} tetramer⁺ CD8⁺ T cells (left) and histograms showing the expression of CD122 and CD25 on indicated populations.

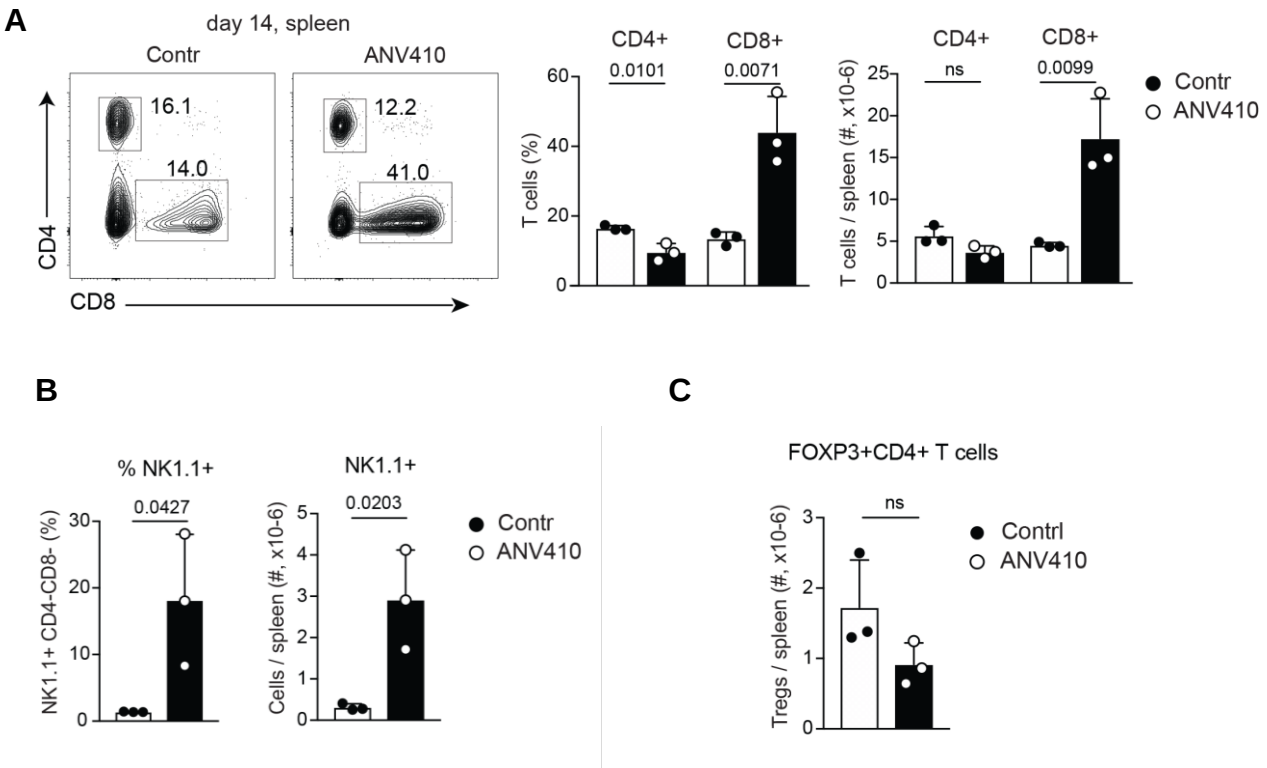

Suppl. Figure 2. Treatment with a CD122-specific IL-2 fusion protein results in CD8 T cell and NK cell but not T_{REG} cell expansion.

C57BL/6 mice were chronically infected with LCMV Docile and receiving intraperitoneal treatment of ANV410 as in Figure 4A (Regimen A).

(**A**) FACS plots (left) and quantifications (right) for total $CD4^+$ or $CD8^+$ T cells.

(**B**) Quantification for $CD3^-NK1.1^+$ NK cells.

(**C**) Quantification for $Foxp3^+$ $CD4^+$ T_{REG} cells.